LABORATORI NAZIONALI DI FRASCATI
SIS – Pubblicazioni

LNF-95/004 (IR)
6 Febbraio 1995

Polarization Effects in Electron Compton Scattering

D. Babusci, G. Giordano, G. Matone

INFN – Laboratori Nazionali di Frascati, P.O. Box 13, I 00044–Frascati (Roma) Italy

Abstract

In this paper we present the full calculation of the final photon polarization in the Compton scattering on electron $\vec{\gamma} + \vec{e} \to \vec{\gamma} + e$. We claim to be in disagreement with some of the results quoted in Ref. [4].

PACS.: 14.20.Ds, 13.88+e, 29.27.Hj, 42.62.Hk

1 Introduction

A general discussion of the polarization effects in Compton scattering can be found in Ref.[1] and in several other review articles published elsewhere [2, 3, 4, 5]. The polarization of the final photon is of particular relevance for the experiments where high energy polarized photons are produced by backscattering of laser light against high energy electrons in a storage ring [4]. As a matter of fact, since the electron spin-flip amplitude vanishes in the backward direction, the final photons retain almost entirely the initial laser polarization. However, at other angles the photon polarization can change due to the role of orbital angular momentum. The knowledge of the average value of the final photon polarization is essential for any experimental activity with the backscattered photon beam.

After a short summary of the basic theoretical formulas, we derive the expressions of all the quantities of interest in the general case where the initial electron is arbitrarily polarized. In particular we find that some of the final photon polarization parameters quoted by F.R.Arutyunian and V.A.Tumanian in Ref.[4] (in the following referred as AT) are wrong. The correct expressions are presented and discussed.

2 Photon Polarization

The most general state of the photon polarization is elliptical and it can be expressed in terms of the two basic vectors of either circular or linear polarization. If the circular base is chosen, up to an overall phase factor, the electric field of a monochromatic plane wave of frequency ω propagating along the z-direction can be written as follows ($c = 1$):

$$\hat{E} = \frac{\vec{E}}{\mid E \mid} = \left\{ e^{-i\eta} \cos\beta\, \hat{\varepsilon}_+ + e^{i\eta} \sin\beta\, \hat{\varepsilon}_- \right\} e^{i\omega(z-t)} \qquad \hat{\varepsilon}_\pm = \frac{1}{\sqrt{2}} (\hat{x} \pm i\,\hat{y}) \quad (2.1)$$

where β, η are the parameters that describe the elliptical trajectory of the electric field shown in fig.(1). The $d_\pm$-semiaxis are determined by the electric field amplitude and the angle β

$$d_\pm^2 = \frac{\mid \vec{E} \mid^2}{2} (1 \pm \sin 2\beta) \qquad d_+^2 + d_-^2 = \mid \vec{E} \mid^2 \quad (2.2)$$

The Stokes parameters are defined by the following combinations [6]:

$$\begin{aligned} \xi_1 &= 2\, Im\{ (\hat{\varepsilon}_+^* \cdot \hat{E})^* (\hat{\varepsilon}_-^* \cdot \hat{E}) \} = \sin 2\beta \sin 2\eta \\ \xi_2 &= \mid \hat{\varepsilon}_+^* \cdot \hat{E} \mid^2 - \mid \hat{\varepsilon}_-^* \cdot \hat{E} \mid^2 = \cos 2\beta \\ \xi_3 &= 2\, Re\{ (\hat{\varepsilon}_+^* \cdot \hat{E})^* (\hat{\varepsilon}_-^* \cdot \hat{E}) \} = \sin 2\beta \cos 2\eta \end{aligned} \quad (2.3)$$

With the appropriate choice of the values of the parameters β all the cases of interest can be selected (λ is the photon helicity)

- *left circular* ($\lambda = 1$) : $\beta = 0, \pi$

$$\hat{E} = \pm e^{-i\eta}\,\hat{\varepsilon}_+\, e^{i\omega(z-t)} \qquad \vec{\xi} = (0,1,0) \tag{2.4}$$

- *right circular* ($\lambda = -1$) : $\beta = \pm\,\pi/2$

$$\hat{E} = \pm e^{i\eta}\,\hat{\varepsilon}_-\, e^{i\omega(z-t)} \qquad \vec{\xi} = (0,-1,0) \tag{2.5}$$

- *linear* : $\beta = \pi/4$

$$\begin{aligned}\hat{E} &= \frac{1}{\sqrt{2}}\left\{\, e^{-i\eta}\,\hat{\varepsilon}_+ \,+\, e^{i\eta}\,\hat{\varepsilon}_-\,\right\} e^{i\omega(z-t)} \\ &= \left\{\, \cos\eta\,\hat{x} \,+\, \sin\eta\,\hat{y}\,\right\} e^{i\omega(z-t)} \qquad \vec{\xi} = (\sin 2\eta, 0, \cos 2\eta)\end{aligned} \tag{2.6}$$

Once the Stokes parameters are given, it's easy to verify that:

- $(1 \pm \xi_3)/2$ represents the probability to find the polarization directions along the $\hat{x}$ and $\hat{y}$ axis, respectively;

- $(1 \pm \xi_1)/2$ represents the probability to find the polarization directions forming an angle $\pi/4$ and $3\pi/4$ with the $\hat{x}$ axis, respectively;

- $(1 \pm \xi_2)/2$ represents the probability for states with helicity ± 1.

Moreover, the linear (P_l), circular (P_c) and total (P) degrees of polarization are defined as follows:

$$P_l = \sqrt{\xi_1^2 + \xi_3^2}\,, \qquad P_c = |\,\xi_2\,|\,, \qquad P = \sqrt{P_l^2 + P_c^2} \tag{2.7}$$

For the monochromatic plane wave (2.1). eqs.(2.3) yield:

$$P_l = |\,\sin 2\beta\,|\,, \qquad P_c = |\,\cos 2\beta\,|\,, \qquad P = 1 \tag{2.8}$$

In the case of a partially polarized plane wave ($P < 1$) the espressions (2.3) give now the quantities ξ_k/P and eq.(2.8) becomes:

$$P_l = P\,|\,\sin 2\beta\,|\,, \qquad P_c = P\,|\,\cos 2\beta\,| \tag{2.9}$$

For further reference, we note that under rotation of an angle ϕ of the $(\hat{x}, \hat{y})$-axis, the Stokes parameters transform according to:

$$\begin{aligned}\xi_1' &= \xi_1\,\cos 2\phi \,-\, \xi_3\,\sin 2\phi \\ \xi_3' &= \xi_1\,\sin 2\phi \,+\, \xi_3\,\cos 2\phi\end{aligned} \tag{2.10}$$

3 The Compton Process

The kinematics of the process is shown in fig.(2) with the usual definitions of the (s,t,u)-variables:

$$\begin{aligned} s - m^2 &= \tilde{s} = 2pk \\ t &= -2kk' \qquad\qquad (\tilde{s}+t+\tilde{u}=0) \\ u - m^2 &= \tilde{u} = -2pk' \end{aligned} \tag{3.1}$$

The process can be conveniently discussed by introducing the Stokes parameters of the incoming photon ($\xi_k^{(i)}$) and those associated with the polarization detector (σ_k). The general expression for the squared amplitude is [1]:

$$\mid \mathcal{M} \mid^2 = 8\pi^2 e^4 \sum_{i=0}^{5} M_i \tag{3.2}$$

where

$$\begin{aligned} M_0 &= Tr\{\rho' Q_0 \rho Q_0 + (\rho' \vec{Q}) \cdot (\rho \vec{Q}')\} \\ M_1 &= Tr\{(\vec{\psi} + \vec{\xi}^{(i)}) \cdot (\rho' Q_0 \rho \vec{Q}' + \rho' \vec{Q} \rho Q_0)\} \\ M_2 &= i\, Tr\{(\vec{\psi} - \vec{\xi}^{(i)}) \cdot (\rho' \vec{Q}) \times (\rho \vec{Q}')\} \\ M_3 &= Tr\{(\vec{\psi} \cdot \vec{\xi}^{(i)})(\rho' Q_0 \rho Q_0 - (\rho' \vec{Q}) \cdot (\rho \vec{Q}')\} \\ M_4 &= Tr\{\rho' (\vec{\psi} \cdot \vec{Q}) \rho (\vec{\xi}^{(i)} \cdot \vec{Q}') + \rho' (\vec{\xi}^{(i)} \cdot \vec{Q}) \rho (\vec{\psi} \cdot \vec{Q}')\} \\ M_5 &= i\, Tr\{(\vec{\psi} \times \vec{\xi}^{(i)}) \cdot (\rho' Q_0 \rho \vec{Q}' - \rho' \vec{Q} \rho Q_0)\} \end{aligned} \tag{3.3}$$

The Stokes "vectors"

$$\vec{\xi}^{(i)} = (\xi_1^{(i)}, \xi_2^{(i)}, \xi_3^{(i)}), \qquad \vec{\psi} = (-\sigma_1, -\sigma_2, \sigma_3) \tag{3.4}$$

are referred to the unit vectors:

$$\hat{\chi}_1^{(i)} = \frac{\vec{k} \times \vec{k}'}{\mid \vec{k} \times \vec{k}' \mid}, \qquad \hat{\chi}_2^{(i)} = \frac{\vec{k} \times \hat{\chi}_1^{(i)}}{\mid \vec{k} \times \hat{\chi}_1^{(i)} \mid} \tag{3.5}$$

and the vectors

$$\vec{Q} = (Q_1, Q_2, Q_3), \qquad \vec{Q}' = (-Q_1, -Q_2, Q_3) \tag{3.6}$$

are defined by ($\not{p} = p_\mu \gamma^\mu$)

$$\begin{aligned} Q_0 &= -ma_+, & Q_1 &= \frac{i}{2} a_+ \gamma_5 \not{K} \\ Q_2 &= -ma_+ \gamma_5, & Q_3 &= ma_+ + \frac{1}{2} a_- \not{K} \\ a_\pm &= \frac{1}{\tilde{s}} \pm \frac{1}{\tilde{u}}, & K &= k + k' \end{aligned} \tag{3.7}$$

In eqs.(3.3) ρ and ρ' are the density matrices of the initial and final electrons, respectively. If the initial electron is polarized but its final polarization remains undetected, we have:

$$\rho = \frac{1}{2}(\not{p} + m)(1 - \gamma_5 \not{\psi}) \qquad \rho' = \frac{1}{2}(\not{p}' + m) \tag{3.8}$$

where, by indicating with $\vec{\zeta}/2$ the average spin of the initial electron in the **ERF** (electron rest frame) system, the 4-vector w satisfies the conditions

$$w_\mu p^\mu = 0\,, \qquad w_\mu w^\mu = -\vec{\zeta}^2$$

In the **LAB**-system, where the electron has momentum $\vec{p}$, one has:

$$w^0 = \frac{1}{m}(\vec{\zeta}\cdot\vec{p}) \qquad \vec{w} = \vec{\zeta} + \frac{w^0}{E+m}\vec{p} \tag{3.9}$$

The squared amplitude of eq.(3.2) can be written in the following form:

$$|\mathcal{M}|^2 = 16\pi^2 e^4 \{ F_0 + (\vec{\xi}^{(i)}\cdot\vec{F}) + (\vec{\sigma}\cdot\vec{F}') + (\vec{\sigma}\cdot T\vec{\xi}^{(i)}) \} \tag{3.10}$$

where the coefficient F_0 and the components of the vectors $\vec{F}$ and $\vec{F}'$ are given by:

$$F_0 = 4m^2 a_+ (1 + m^2 a_+) - b \qquad \left(b = \frac{\tilde{s}}{\tilde{u}} + \frac{\tilde{u}}{\tilde{s}}\right) \tag{3.11}$$

$$\begin{aligned} F_1 &= 0 & F_1' &= F_1 \\ F_2 &= -2ma_+ \{ (1 + 2m^2 a_+)(kw) + (k'w) \} & F_2' &= F_2(k \leftrightarrow k') \\ F_3 &= -4m^2 a_+ (1 + m^2 a_+) & F_3' &= F_3 \end{aligned} \tag{3.12}$$

and the T-matrix is defined by the following elements:

$$\begin{aligned} T_{11} &= 2(1 + 2m^2 a_+) & T_{22} &= -\frac{b}{2} T_{11} & T_{33} &= 2 - F_3 \\ T_{12} &= \frac{s}{\tilde{u}} T_{21} = -4\frac{m}{\tilde{u}} a_+ \epsilon^{\mu\nu\lambda\eta} p_\mu w_\nu k_\lambda k'_\eta & T_{13} &= T_{31} = 0 \\ T_{23} &= ma_+ \{ 2\frac{\tilde{u}}{\tilde{s}}(kw) + T_{11}(k'w) \} & T_{32} &= ma_+ \{ T_{11}(kw) + 2\frac{\tilde{s}}{\tilde{u}}(k'w) \} \end{aligned} \tag{3.13}$$

Eq.(3.10) can be rewritten in the following form

$$|\mathcal{M}|^2 = \frac{1}{2}\,|\bar{\mathcal{M}}|^2\,\{1 + (\vec{\sigma}\cdot\vec{\xi}^{(f)})\} \tag{3.14}$$

where

$$\vec{\xi}^{(f)} = (\xi_1^{(f)}, \xi_2^{(f)}, \xi_3^{(f)}) = \frac{1}{A_0}\,(\,\vec{F}' + T\vec{\xi}^{(i)}\,) \tag{3.15}$$

is the Stokes "vector" of the final photon referred to the unit vector base

$$\hat{\chi}_1^{(f)} = \hat{\chi}_1^{(i)}\,, \qquad \hat{\chi}_2^{(f)} = \frac{\vec{k}' \times \hat{\chi}_1^{(f)}}{|\,\vec{k}' \times \hat{\chi}_1^{(f)}\,|} \tag{3.16}$$

which should not be confused with that of eq.(3.5) defined for the initial photon. The presence of the scalar product $\vec{\sigma} \cdot \vec{\xi}^{(f)}$ allows to determine the photon flux in any given polarization channel by selecting the appropriate value of the detector Stokes "vector" $\vec{\sigma}$ in eq.(3.14). Moreover, by putting $\vec{\sigma} = 0$ in eq.(3.10) and multiplying by 2 the result, one obtains the squared amplitude summed over the polarizations of the final photon

$$|\,\bar{\mathcal{M}}\,|^2 = 32\pi^2 e^4\,\{\,F_0 + (\,\vec{\xi}^{(i)} \cdot \vec{F}\,)\} = 32\pi^2 e^4\,A_0 \tag{3.17}$$

3.1 The ERF System

In this system the calculations of the coefficient F_0, the components of the vector $\vec{F}$ and the T-matrix elements, greatly simplify. With the positions

$$\nu = \frac{|\,\vec{k}\,|}{m}\,, \quad \nu' = \frac{|\,\vec{k}'\,|}{m}$$

and by indicating with θ the angle between the incoming and outgoing photons, one has:

$$\tilde{s} = 2m^2\nu \qquad \tilde{u} = -2m^2\nu' \tag{3.18}$$
$$\nu' = \frac{\nu}{1 + \nu(1 - \cos\theta)}$$

Eqs.(3.15) become:

$$\begin{aligned}
\xi_1^{(f)} &= \frac{1}{A_0}\,\{\,2\,\xi_1^{(i)}\,\cos\theta + \xi_2^{(i)}\,\nu(1-\cos\theta)\,(\vec{h}\cdot\vec{\zeta}\,)\,\} \\
\xi_2^{(f)} &= \frac{1}{A_0}\,\Big\{ -\nu(1-\cos\theta)\,(\vec{f}\,'\cdot\vec{\zeta}\,) - \xi_1^{(i)}\,\nu'(1-\cos\theta)\,(\vec{h}\cdot\vec{\zeta}\,) \\
&\qquad + \xi_2^{(i)}\left(\frac{\nu}{\nu'} + \frac{\nu'}{\nu}\right)\cos\theta - \xi_3^{(i)}\,\nu'(1-\cos\theta)\,(\vec{g}\cdot\vec{\zeta}\,)\Big\} \\
\xi_3^{(f)} &= \frac{1}{A_0}\,\{\,\sin^2\theta + \xi_2^{(i)}\,\nu(1-\cos\theta)\,(\vec{g}\,'\cdot\vec{\zeta}\,) + \xi_3^{(i)}\,(1+\cos^2\theta)\,\}
\end{aligned} \tag{3.19}$$

where

$$A_0 = \left(\frac{\nu}{\nu'} + \frac{\nu'}{\nu} - \sin^2\theta\right) + \xi_3^{(i)} \sin^2\theta - \xi_2^{(i)} \nu(1-\cos\theta)\,(\vec{f}\cdot\vec{\zeta}) \qquad (3.20)$$

and

$$\begin{aligned} \vec{f} &= \hat{k}\cos\theta + \hat{k}'\frac{\nu'}{\nu} \quad , \quad \vec{f}' = \hat{k} + \hat{k}'\frac{\nu'}{\nu}\cos\theta \\ \vec{g} &= \hat{k} - \hat{k}'\cos\theta \quad , \quad \vec{g}' = \hat{k}\cos\theta - \hat{k}' \\ \vec{h} &= \hat{k}\times\hat{k}' \end{aligned} \qquad (3.21)$$

Following eq.(3.17), the cross-section averaged over the polarization states of the final photon becomes ($r_0 = e^2/m$):

$$\frac{d\sigma}{d\Omega} = \frac{r_0^2}{2}\left(\frac{\nu'}{\nu}\right)^2 A_0 \qquad (3.22)$$

that is the usual Klein-Nishina formula [1, 2, 3].

3.1.1 Unpolarized Electrons

In the case $\vec{\zeta} = 0$ eqs.(3.19,3.20) specialize into the known expressions:

$$\begin{aligned} \xi_1^{(f)} &= \xi_1^{(i)}\,\frac{2\cos\theta}{A_0} \\ \xi_2^{(f)} &= \xi_2^{(i)}\,\frac{\cos\theta}{A_0}\left(\frac{\nu}{\nu'} + \frac{\nu'}{\nu}\right) \\ \xi_3^{(f)} &= \frac{1}{A_0}\left\{\sin^2\theta + \xi_3^{(i)}\,(1+\cos^2\theta)\right\} \end{aligned} \qquad (3.23)$$

where A_0 is given by

$$A_0 = \left(\frac{\nu}{\nu'} + \frac{\nu'}{\nu} - \sin^2\theta\right) + \xi_3^{(i)} \sin^2\theta \qquad (3.24)$$

The same expressions are reported in eqs.(3.13) of Ref.[4] and can be compared with ours by renaming the indices: $(1,2,3)_{AT} \rightarrow (3,1,2)$). The components $\xi_1^{(f)}$ and $\xi_3^{(f)}$ are identical and thus, we completely agree with Ref.[4] when the photons are linearly polarized. On the contrary, the AT-value for $\xi_2^{(f)}$ is:

$$\xi_2^{(f)}\,|_{AT} = \frac{\cos\theta}{A_0}\left\{\left(\frac{\nu}{\nu'} + \frac{\nu'}{\nu} - 2\right)\xi_1^{(i)} + 2\xi_2^{(i)}\right\} \qquad (3.25)$$

which is incorrect because it allows for a circular polarization component of the final

photon even when the initial photon is purely linear ($\xi_2^{(i)} = 0$). A typing error is possible but not consistent with the rest of the AT-paper.

According to eqs.(3.23,3.24), the Stokes parameters do not show any explicit dependence upon the ϕ-emission angle of the final photon. As a matter of fact, this dependence is only hidden in the expressions of the unit vectors $\hat{\chi}_{1,2}^{(i)}$ and $\hat{\chi}_{1,2}^{(f)}$. In the reference system where the kinematics of the process has been defined (the z-axis is along the incoming photon momentum), these expressions are:

$$\begin{aligned} \hat{\chi}_1^{(i)} &= (-\cos\phi,\, \sin\phi,\, 0) \qquad & \hat{\chi}_2^{(i)} &= (-\sin\phi,\, -\cos\phi,\, 0) \\ \hat{\chi}_1^{(f)} &= \hat{\chi}_1^{(i)} & \hat{\chi}_2^{(f)} &= (-\cos\theta\,\sin\phi,\, -\cos\theta\,\cos\phi,\, \sin\theta) \end{aligned} \tag{3.26}$$

By rotating these two sets of unit vectors of an angle ϕ, at constant θ, one obtains (see eq.(2.10)):

$$\begin{aligned} s_1^{(f)} = \pm\frac{1}{A_0}\Big\{ &-\sin^2\theta\sin 2\phi + s_1^{(i)}\left[(1\mp\cos\theta)^2\sin^2 2\phi \pm 2\cos\theta\right] \\ &- \frac{1}{2}\,s_3^{(i)}\left[(1\mp\cos\theta)^2\sin 4\phi\right]\Big\} \\ s_2^{(f)} = s_2^{(i)}\,\frac{\cos\theta}{A_0}\left(\frac{\nu}{\nu'}+\frac{\nu'}{\nu}\right) \\ s_3^{(f)} = \frac{1}{A_0}\Big\{ &\sin^2\theta\cos 2\phi + \frac{1}{2}\,s_1^{(i)}\left[(1\mp\cos\theta)^2\sin 4\phi\right] \\ &+ s_3^{(i)}\left[(1\mp\cos\theta)^2\cos^2 2\phi \pm 2\cos\theta\right]\Big\} \end{aligned} \tag{3.27}$$

with A_0 given by

$$A_0 = \left(\frac{\nu}{\nu'}+\frac{\nu'}{\nu} - \sin^2\theta\right) + (s_1^{(i)}\cos 2\phi + s_3^{(i)}\sin 2\phi)\,\sin^2\theta \tag{3.28}$$

The Stokes parameters $\vec{s}^{(i)}$ and $\vec{s}^{(f)}$ are expressed in terms of two reference bases perpendicular to the corresponding photon momentum. The unit vectors defined for the initial photon coincides with those $\hat{x}$ and $\hat{y}$ of the reference system, whereas those of the final photon depend upon θ. The double sign corresponds to the emission of the final photon in the forward (upper sign) and backward (lower sign) emisphere, respectively. Since eqs. (3.5,3.16) assume that the third axis is oriented along the photon momentum and the unit vector $\hat{\chi}_2^{(f)}$ changes direction under reflection (see eq.(3.26)), the final photon turns out to be described in systems with opposite handness when is emitted forward or backward. This explains why the ϕ-dependence has to be taken with opposite signs when the photon is emitted in the two emispheres. As for the circular polarization no ϕ-dependence is expected. Hence, no double sign appear in the expression for $s_2^{(f)}$ and a circularly polarized photon changes helicity passing from one emisphere to the other.

On the experimental side, the final size of any practical detector requires to perform an integration over its finite ϕ-acceptance. By weighing eqs.(3.27) with the

differential cross section and averaging over the full ϕ-range

$$< \vec{s}^{(f)} > = \frac{\int_0^{2\pi} d\phi \, A_0 \vec{s}^{(f)}}{\int_0^{2\pi} d\phi \, A_0} = \frac{\int_0^{2\pi} d\phi \, A_0 \vec{s}^{(f)}}{< A_0 >} \tag{3.29}$$

one has:

$$\begin{aligned} < s_1^{(f)} > &= \pm s_1^{(i)} \frac{(1+|\cos\theta|)^2}{2 < A_0 >} \\ < s_2^{(f)} > &= s_2^{(i)} \frac{\cos\theta}{< A_0 >} \left(\frac{\nu}{\nu'} + \frac{\nu'}{\nu} \right) \\ < s_3^{(f)} > &= s_3^{(i)} \frac{(1+|\cos\theta|)^2}{2 < A_0 >} \end{aligned} \tag{3.30}$$

where

$$< A_0 > = \frac{\nu}{\nu'} + \frac{\nu'}{\nu} - \sin^2\theta \tag{3.31}$$

Fig.(3) shows the behaviour of the Stokes parameters of the final photon as function of the ratio $\alpha = \nu'/\nu'_{max}$, when UV-photons from a frequency quadrupled $Nd-YAG$ laser with $\lambda = 266\ nm$ $(4.66\ eV)$ collide against the electrons of the up-graded $NSLS$ X-ray ring at BNL $(E_e = 2.8\ GeV)$ [8]. This behaviour can be understood from the analysis of the kinematical term appearing in eqs.(3.30,3.31). This factor can be rewritten as follows:

$$\frac{\nu}{\nu'} + \frac{\nu'}{\nu} = 2 + \frac{\nu^2(1-\cos\theta)^2}{1 + \nu(1-\cos\theta)} \tag{3.32}$$

and, for $\nu \simeq 1$ (as in fig.(3)) is always very close to 2, in the whole angular range. According to eqs.(3.30,3.31) the photons emitted inside the two cones centered around the $\theta = 0$ ($\alpha = 1$) and $\theta = \pi$ ($\alpha = 0.883$, in the kinematical case considered in fig.(3)), retain the same degree of polarization of the initial photon. The cusp, present only in the case of linearly polarized photons (see fig.(3a)), occurs at $\theta = \pi/2$ as consequence of the absolute value appearing in eqs.(3.30). In the case of incoming circularly polarized light (see fig.(3b)), the final photon mantains the helicity in forward emisphere but scatters with opposite helicity in the backward emisphere. In both cases, the behaviour of the polarization degree as a function of the scattering energy, is identical.

In the region $\nu \geq 1$, the kinematical factor of eq.(3.32) increases with ν, giving rise to a corresponding decrease of the degree of linear polarization of the final photon. Fig.(4a) shows that the drop of the linear polarization is dramatic when the electrons are in the multi-GeV region. This drives to the surprising conclusion that laser backscattering, at very high energy, can not be considered as a good source of linearly polarized photons.

Thanks to the cancellation of the kinematical factor (3.32) in the second of eqs.(3.30) at $\theta = 0, \pi$, this effect does not indeed occur for circularly polarized photons, as shown in fig.(4b). This is clearly expected from angular momentum considerations, but disagrees quite strongly with the corresponding AT-result (third of

eqs.(3.25) of Ref. [4]):

$$< s_2^{(f)} >|_{AT} = s_2^{(i)} \frac{2\cos\theta}{< A_0 >} \tag{3.33}$$

Here a fully circularly polarized photon is predicted to bounce back from the electron with a degree of circular polarization that, despite the angular momentum conservation, decreases with the increasing energy.

3.1.2 Polarized Electrons

With the help of eqs.(3.19,3.20) we can extend these considerations to the case where the electrons are polarized either longitudinally or transversly to the direction of the incoming photon: any other polarization state can be reconduced to a combination of these two basic states.

The electrons in a storage ring can build up a partial transverse polarization as a result of the combined action of the polarizing synchrotron radiation and the depolarizing effect due to the magnetic lattice imperfections. The $\vec{\zeta}$-dependent term in eqs.(3.20) shows that the electron transverse polarization can be measured with circularly polarized photons, by looking at the ϕ-asimmetry in the distribution of the scattered photons. This opportunity has been repeatedly used to measure the electron transverse polarization in several storage rings (SPEAR, LEP, HERA) [7]. In the case where the electron polarization vector is along the y-axis $[\zeta = (0, P_e, 0)]$, by assuming that $\phi = 0$ corresponds to the positive direction of this axis, we can define the following up-down asymmetry:

$$\begin{aligned}\Sigma &= \frac{A_0(\phi=0) - A_0(\phi=\pi)}{A_0(\varphi=0) + A_0(\phi=\pi)} = \frac{1}{2}\frac{A_0(\phi=0) - A_0(\phi=\pi)}{< A_0 >} \\ &= -\xi_2^{(i)} P_e \frac{\nu\,(1-\cos\theta)\,\sin\theta}{(1+\cos^2\theta)\,[1+\nu\,(1-\cos\theta)] \;+\; \nu^2\,(1-\cos\theta)^2}\end{aligned} \tag{3.34}$$

The behaviour of this asymmetry as a function of the scattering angle for three different values of ν is shown in fig.(5). Let's note that the ν-dependance of this quantity changes considerably in the low and high energy regimes

$$\begin{aligned}\nu \ll 1 \qquad \Sigma &\approx -\xi_2^{(i)} P_e\, \nu \frac{(1-\cos\theta)\,\sin\theta}{1+\cos^2\theta} \\ \nu \gg 1 \qquad \Sigma &\approx -\xi_2^{(i)} P_e \frac{1}{\nu}\frac{\sin\theta}{1-\cos\theta}\end{aligned} \tag{3.35}$$

However, the ϕ-averaged polarization of the final photon is completely insensitive to the electron transverse polarization.

The greatest interest arises when the electrons are longitudinally polarized. First of all, fig.(6) shows that unpolarized photons acquire some small degree of circular polarization ($\approx$ 20 %) when they are scattered off longitudinally polarized electrons. When the laser photons are circular, fig.(7a) shows that the electron helicity states

determine different values for the circular polarization of the final photons, as reported also in Ref. [5]. This difference amplifies considerably at high energy [see fig.(7b)].

3.2 The LAB System

On the experimental side it's definetely more convenient to look at the photon polarization in the **LAB**-system, where the real experiments are performed. However in this system the formalism discussed in sec.3 can not be handled as easily as it has been in the **ERF**-system and therefore we will limit ourselves to report some of the most interesting results of our analysis.

3.2.1 Unpolarized Electrons

Fig.(8) shows the behaviour of the linear and circular polarization of the LEGS photons, when the electron are unpolarized. Let us notice first that the value $\alpha = 1$ corresponds to backward scattering in the **LAB** but to forward scattering in the **ERF**-system. The Lorentz transformation that connects the two system is such that the cusp profile seen in fig.(3a) is so squeezed against the vertical axis that is not visible in fig.(8a). This result would be in strong disagreement with that of Ref.[4], if these authors really claim that the polarization profile is unaffected by the Lorentz transformation. And, indeed, this seems to be the case: the energy scale along the abscissa indicates that fig.(22) of Ref.[4] refers to the **LAB**-system and the reported polarization degree exhibits the same cusp-like behaviour that we found in the **ERF**-system [see fig.(3a)]. However, this evident inconsistency doesn't show up in the backward direction where the LEGS-type of experiments usually operate. It would appear as a huge effect only for $\theta < \pi/2$. At present, no data are available to disentangle this question.

Fig.(9) shows the transverse spatial distribution of the backscattered photons in the present LEGS conditions: linearly polarized light against unpolarized electrons. According with the structure of the Klein-Nishina formula, the two dips, clearly visible in fig.(9), line-up with the polarization direction of the initial photons and disappear completely in fig.(10) where the same distribution is shown for circular photons.

3.2.2 Polarized Electrons

Fig.(11) shows the asymmetry defined in eq.(3.34) as seen in the **LAB**-system, expressed in terms of the angular offset respect to the backward direction.

Similarly to what has been found in **ERF**-system, the effect of the electron transverse polarization on the ϕ-averaged polarization vanishes. The interest is mostly concentrated in the case of circular photons and longitudinally polarized electrons. Here the cross section of eq.(3.17) depends explicitly on the relative orientation of the photon and electron spins: fig.(12) shows how fig.(7a) is modified under the effect of the Lorentz transformation.

4 Laser Light Polarization Measurement

A possible set-up for the polarization measurement at LEGS is shown in fig.(13). The photon beam impinges upon a quarter-wave plate that rotates at a constant angular speed Ω. After the plate, a polarization analyzer separates the x and y components of the electric field and the two intensities are monitorized by two photodiode detectors. The quarter-wave plate introduces a 90^0 dephasing into the polarization component that lies along its fundamental axis and leaves the perpendicular component untouched.

Let us consider the general expression for an incoming elliptical beam given by eq.(2.1)

$$\hat{E} = \left\{ E_x \, \hat{x} + E_y \, \hat{y} \right\} e^{i\omega(z-t)} \tag{4.1}$$

where

$$E_x = \frac{1}{\sqrt{2}} \left(e^{-i\eta} \cos\beta + e^{i\eta} \sin\beta \right) \qquad E_y = \frac{i}{\sqrt{2}} \left(e^{-i\eta} \cos\beta - e^{i\eta} \sin\beta \right) \tag{4.2}$$

It can be shown that after the rotating plate, the electric field components become:

$$\begin{pmatrix} E'_x \\ E'_y \end{pmatrix} = W(t) \begin{pmatrix} E_x \\ E_y \end{pmatrix} = \frac{1-i}{2} \begin{pmatrix} i - \cos 2\Omega t & \sin 2\Omega t \\ \sin 2\Omega t & i + \cos 2\Omega t \end{pmatrix} \begin{pmatrix} E_x \\ E_y \end{pmatrix} \tag{4.3}$$

and the corresponding intensities are:

$$\begin{aligned} |\, E'_x \,|^2 &= \frac{1}{2} \left\{ 1 + \xi_2 \sin 2\Omega t + \frac{1}{2} \left[\xi_3 (1 + \cos 4\Omega t) - \xi_1 \sin 4\Omega t \right] \right\} \\ |\, E'_y \,|^2 &= \frac{1}{2} \left\{ 1 - \xi_2 \sin 2\Omega t - \frac{1}{2} \left[\xi_3 (1 + \cos 4\Omega t) - \xi_1 \sin 4\Omega t \right] \right\} \end{aligned} \tag{4.4}$$

Both components are modulated at the two frequencies 2Ω and 4Ω ($c = 1$): the former is associated to the circular polarization, the latter to the linear polarization. The amplitudes of these two harmonics can be measured with a Fourier analysis of the two photodiode signals and the Stokes parameters can be completely determined.

Let us consider few standard cases:

- *unpolarized photons* : $\xi = (0, 0, 0)$

$$|\, E'_x \,|^2 = |\, E'_y \,|^2 = \frac{1}{2}$$

- *circularly polarized photons* : $\vec{\xi} = (0, \pm 1, 0)$

$$|\, E'_x \,|^2 = \frac{1}{2} \left(1 \pm \sin 2\Omega t \right) \qquad |\, E'_y \,|^2 = \frac{1}{2} \left(1 \mp \sin 2\Omega t \right)$$

- *linearly polarized photons* :

$$\vec{\xi}=(\pm 1,0,0) \qquad |E'_x|^2=\frac{1}{4}\left(2\mp\sin 4\Omega t\right) \qquad |E'_y|^2=\frac{1}{4}\left(2\pm\sin 4\Omega t\right)$$

$$\vec{\xi}=(0,0,\pm 1) \qquad |E'_x|^2=\frac{1}{4}\left[(2\pm 1)\pm\cos 4\Omega t\right] \qquad |E'_y|^2=\frac{1}{4}\left[(2\mp 1)\mp\cos 4\Omega t\right]$$

In conclusion, in fig.(14) we present the time behaviour of the intensities $|E'_{x,y}|^2$ for an arbitrarily selected Stokes vector. By assuming an angular speed Ω of $12^0 s^{-1}$ (1 turn in 30 seconds), the time scale in fig.(14) spans a time interval of 30 seconds.

References

[1] L.D.Landau, E.M.Lifšits, **Relativistic Quantum Theory**, part 1, p.301, Pergamon Press 1971.

[2] U. Fano, *J. Opt. Soc. Am.*, 39, (1949) 859.

[3] F.W.Lipps, H.A.Tolhoek, *Physica*, XX, (1954) 395.

[4] F.R.Arutyunian, V.A.Tumanian, *Sov. Phys. Usp.*, 83, (1964) 339; *Phys. Lett.* 4, (1963) 177.

[5] Y.S.Tsai, *Phys. Rev.*, D48, (1993) 96.

[6] J.D.Jackson, **Classical Electrodynamics**, 2nd Ed., p.277, Wiley & Sons 1975.

[7] D.B.Gustavson et al., *Nucl. Instr. Meth.*, 165, (1979) 177; L.Knudsen et al., *Phys. Lett.*, B270, (1991) 97 and references quoted therein.

[8] C.E.Thorn et al., *Nucl. Instr. Meth.*, A285, (1989) 447; LEGS-Spin Collaboration (D.Babusci et al.), *BNL-61005* (1994).

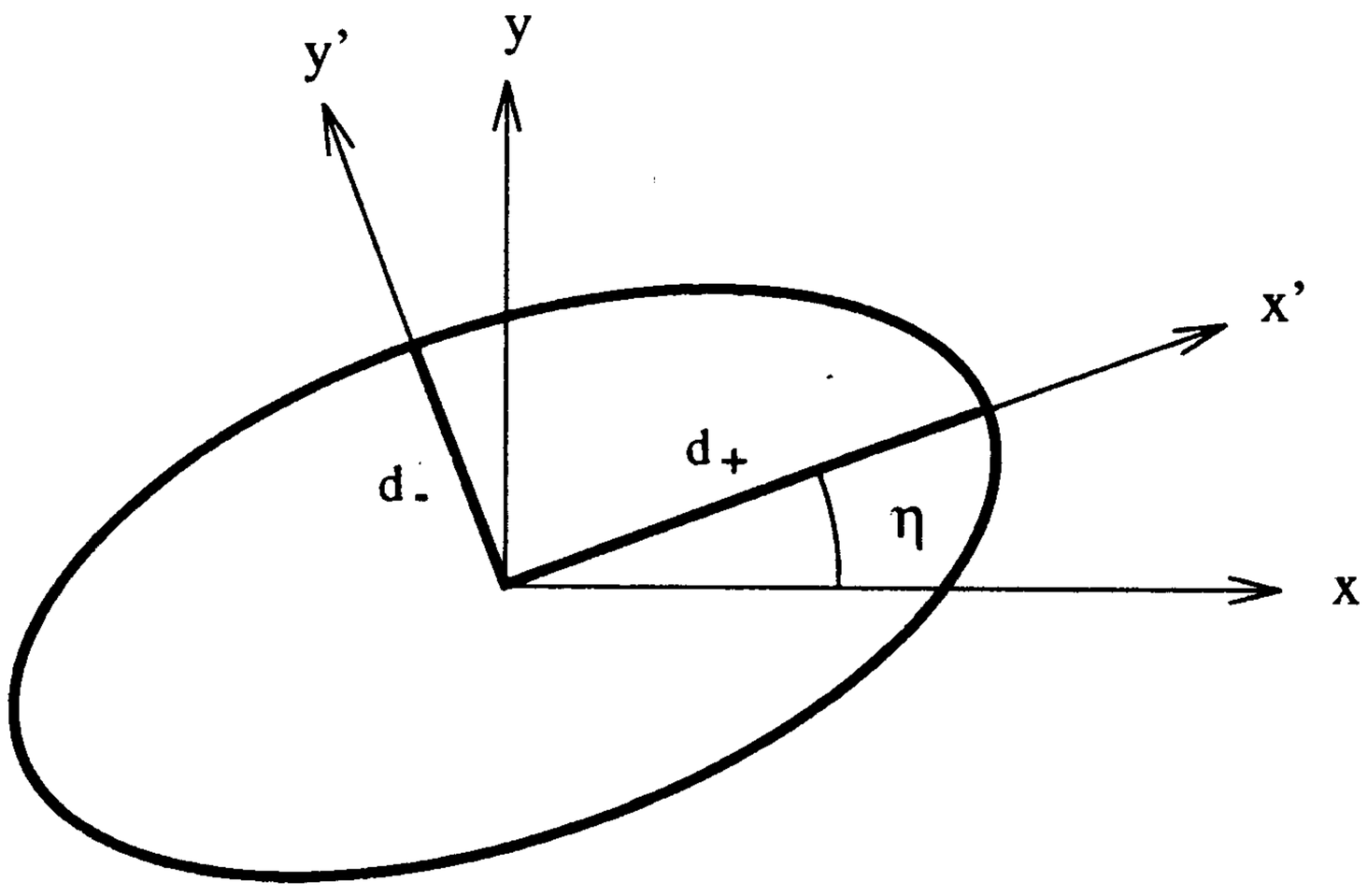

Figure 1: Elliptically polarized plane wave.

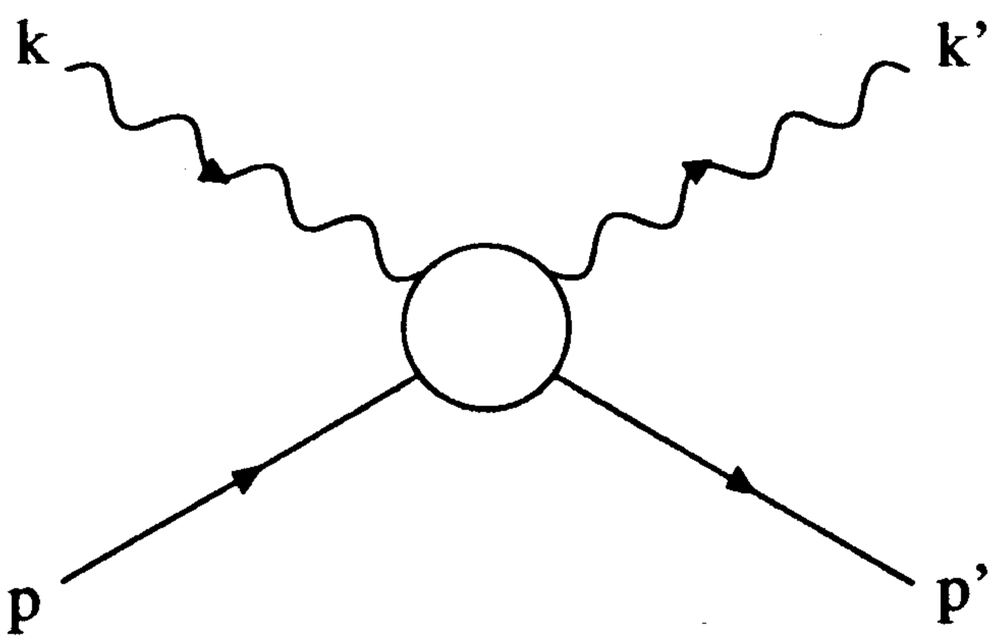

Figure 2: Kinematics of the Compton process.

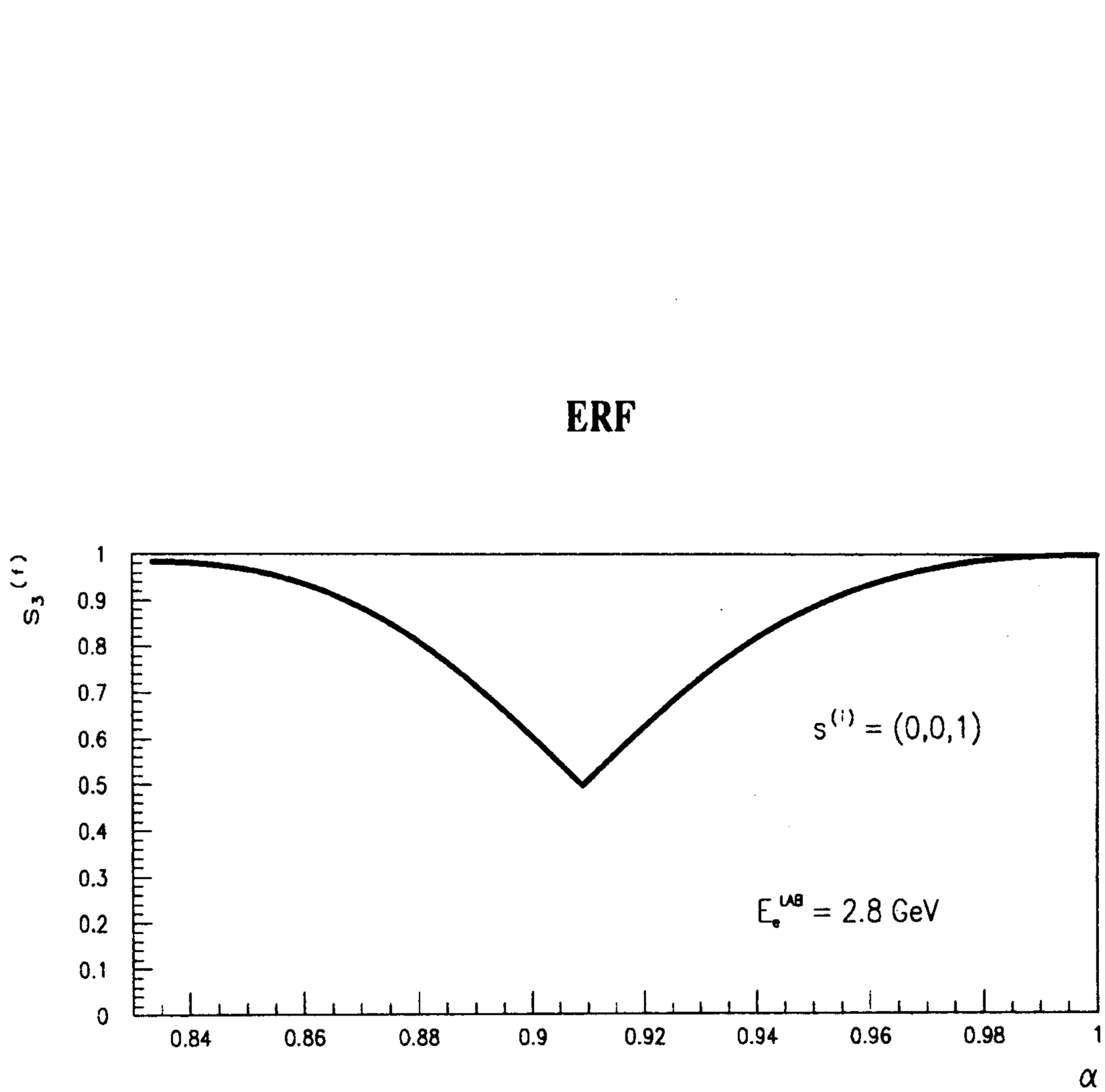

Figure 3: Stokes parameters of the final photon as function of $\alpha = \nu'/\nu'_{max}$ in the **ERF**-system: *a*) s_3 for linearly polarized incident photon $\vec{s}^{(i)} = (0,0,1)$; *b*) s_2 for circularly polarized incident photon $\vec{s}^{(i)} = (0,1,0)$. The electron energy in the **LAB**-system is 2.8 GeV ($\nu = 0.1$).

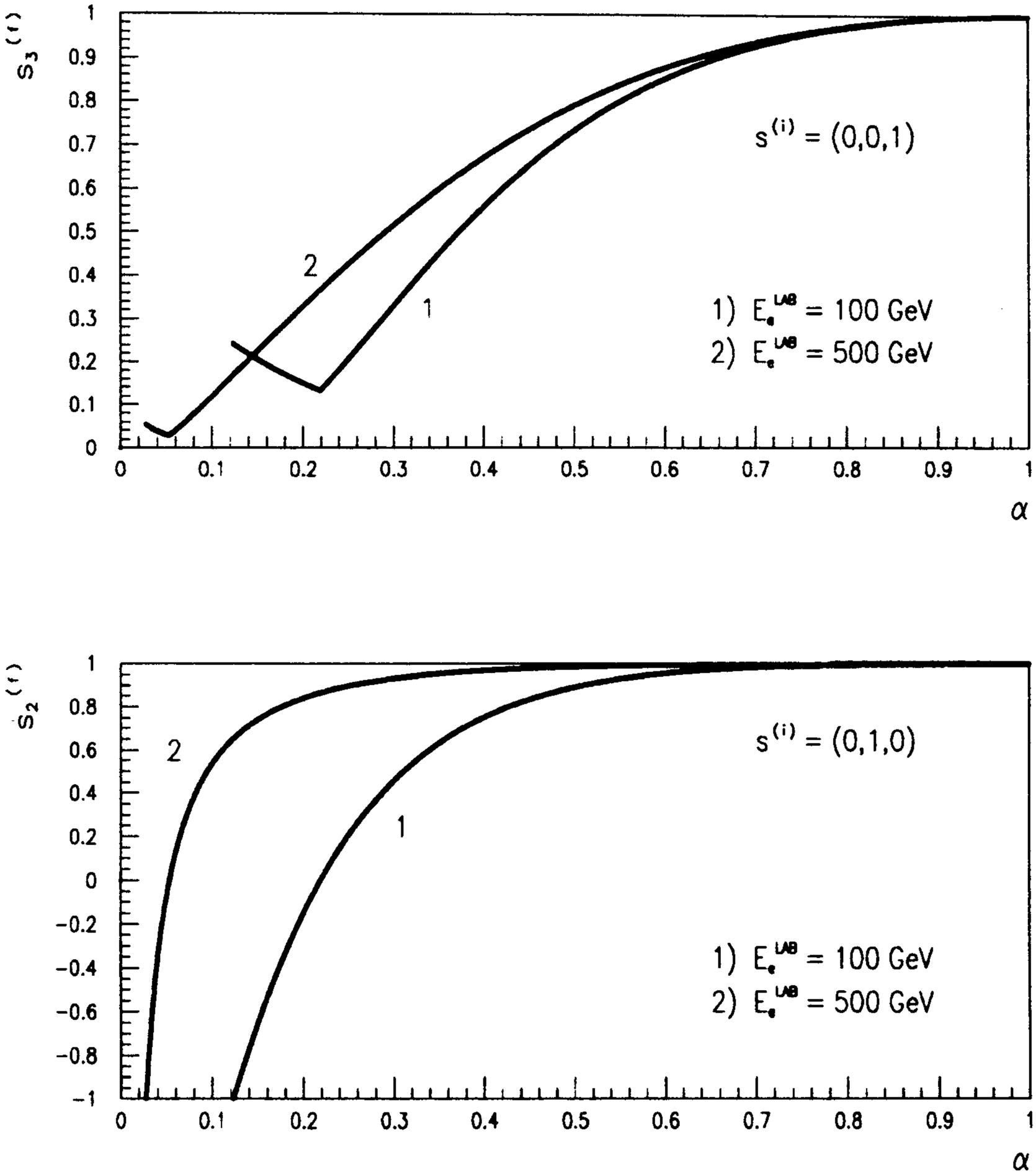

Figure 4: The same of fig.(3) for two different values of the energy of the initial electron in the **LAB**-system.

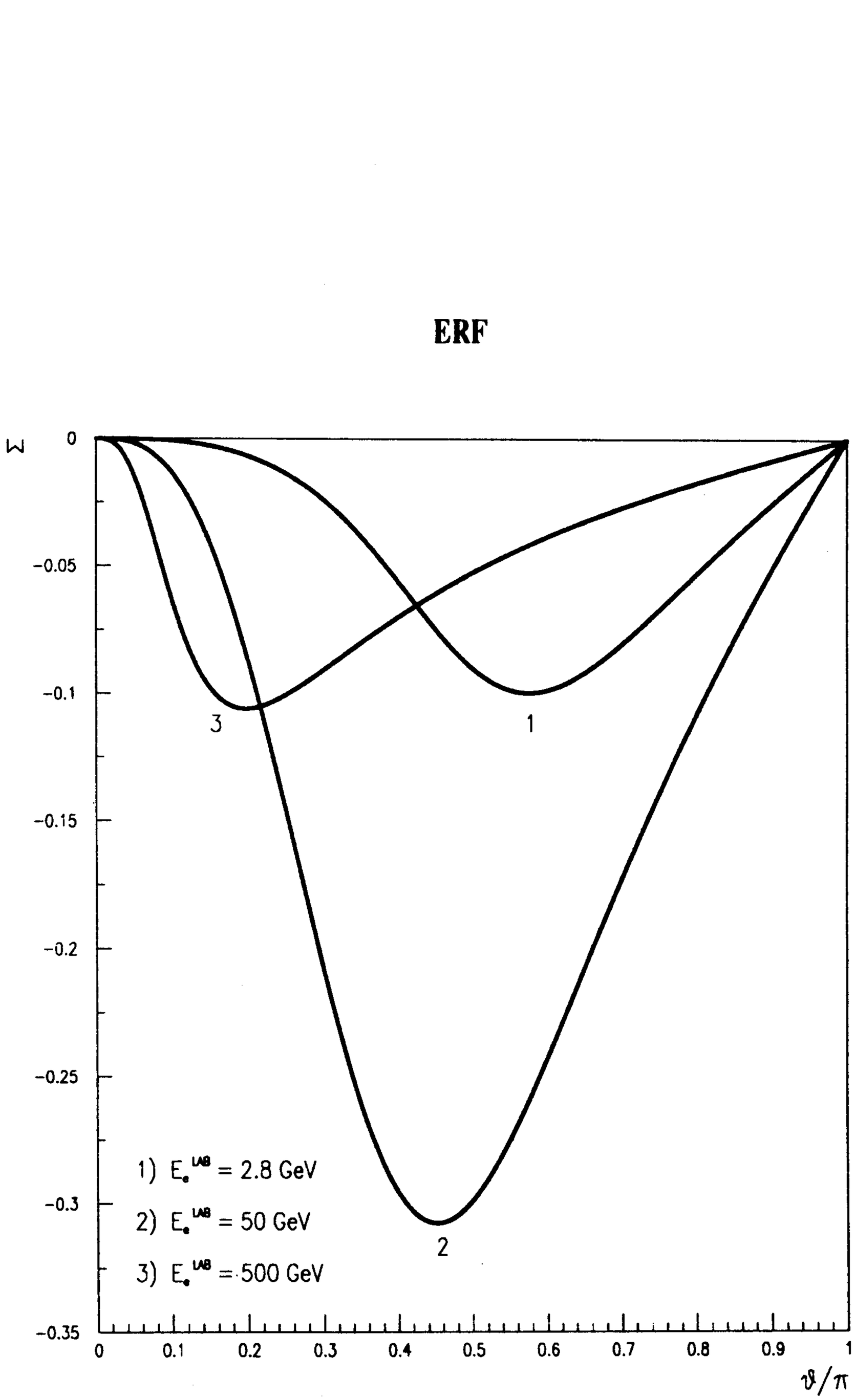

Figure 5: Up-down asymmetry of eq.(3.34) as function of the scattering angle in units of π in the **ERF**-system, for three different values of the energy of the electron in the **LAB**-system.

ERF

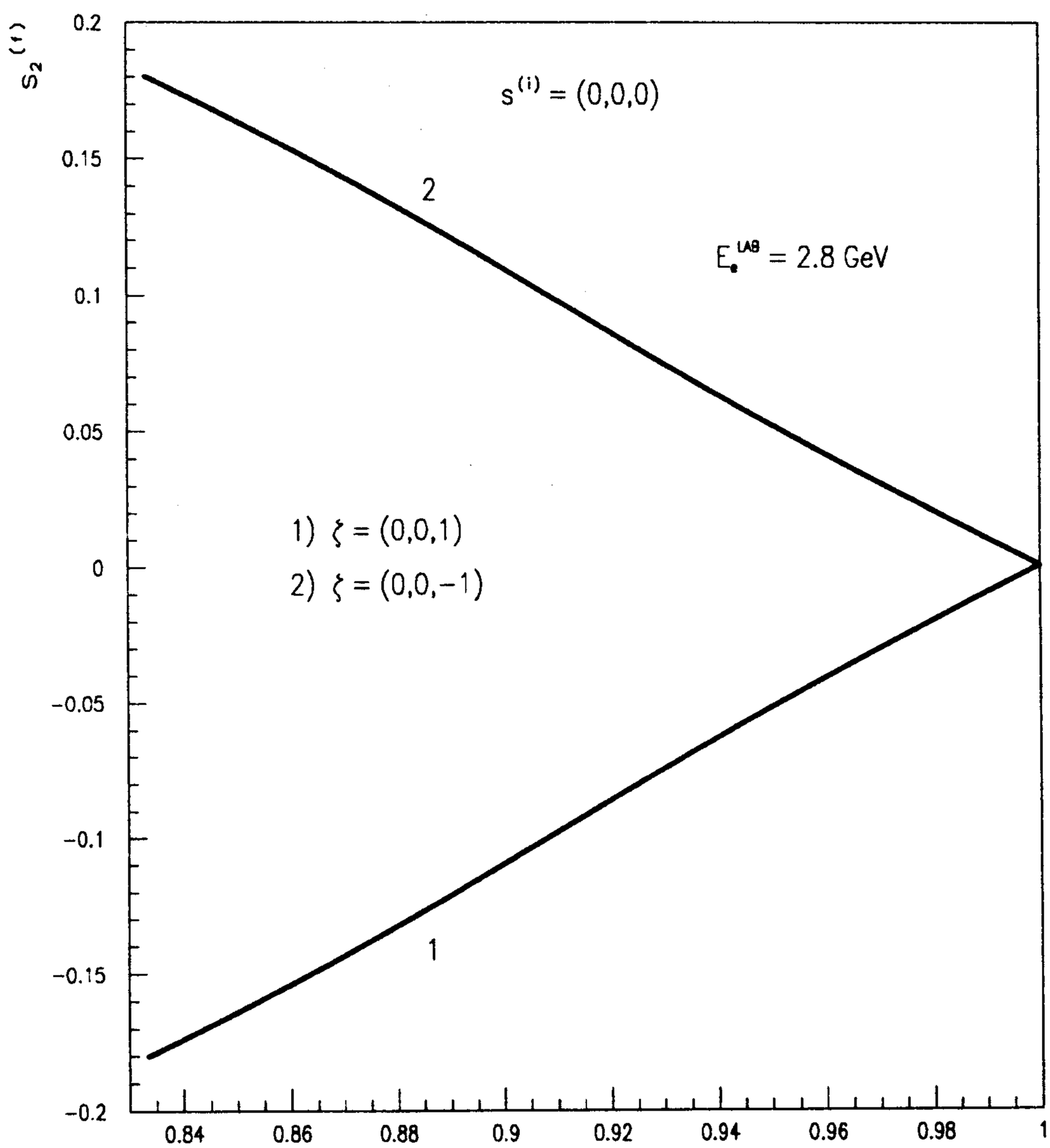

Figure 6: $s_2^{(f)}$ in the **ERF**-system for unpolarized incoming photon ($\vec{s}^{(i)} = 0$) and longitudinally polarized electrons: 1) $\vec{\zeta} = (0,0,1)$; 2) $\vec{\zeta} = (0,0,-1)$.

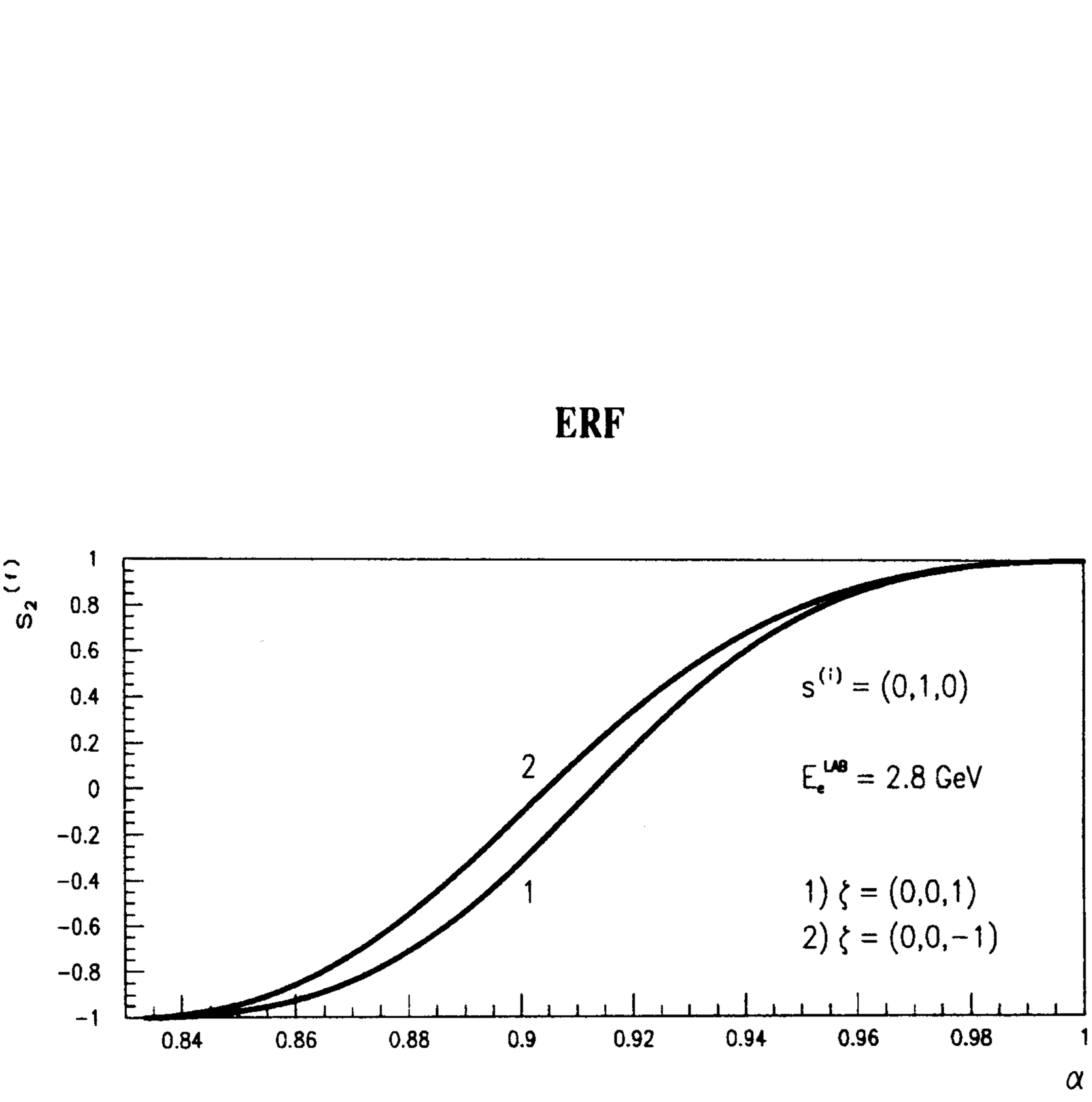

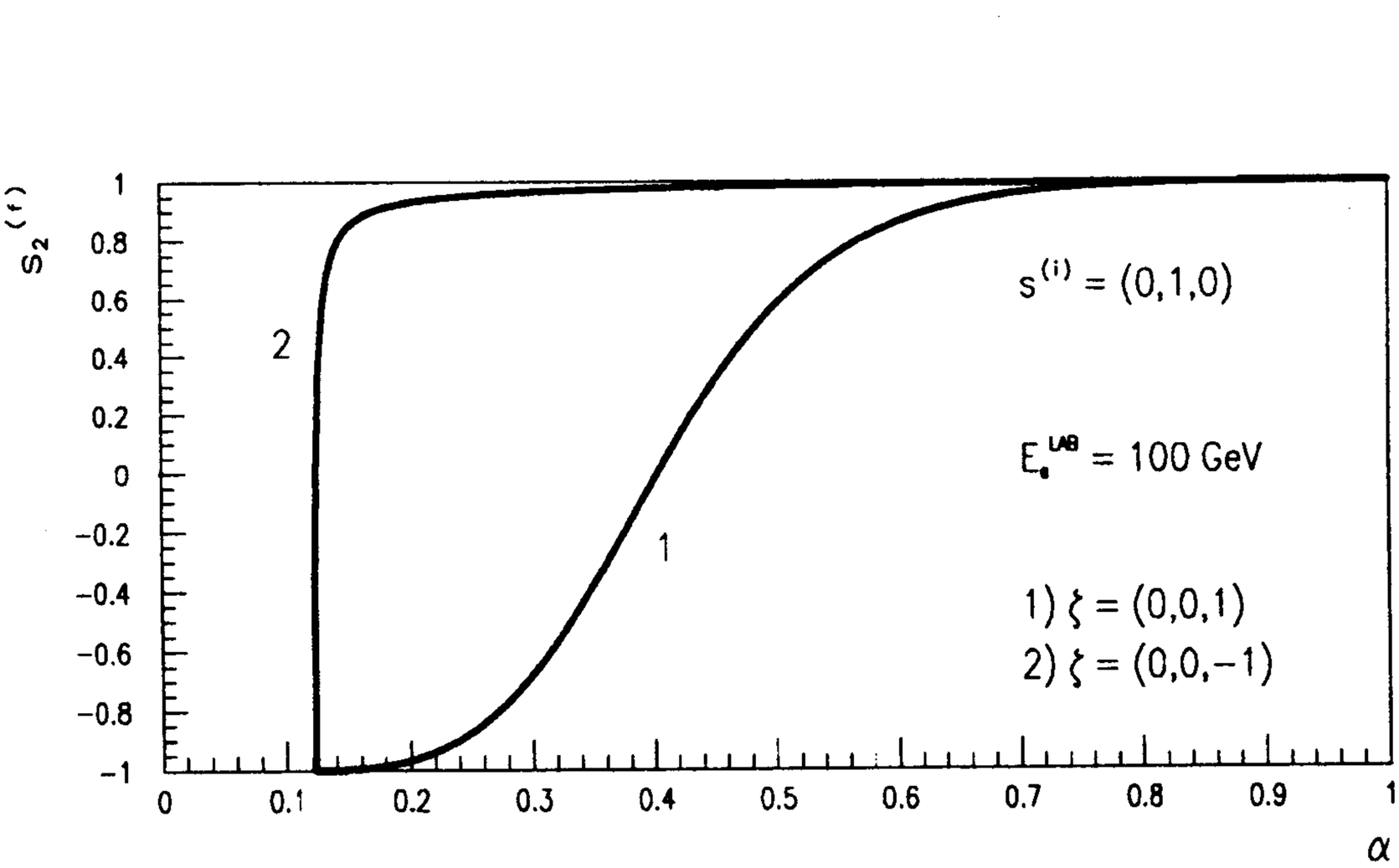

Figure 7: The same of fig.(6) in the case of circularly polarized incoming photon ($\vec{s}^{(i)} = (0,1,0)$), for two different values of the energy of the initial electron in the **LAB**-system.

LAB

Figure 8: The same of fig.(3) in the **LAB** system.

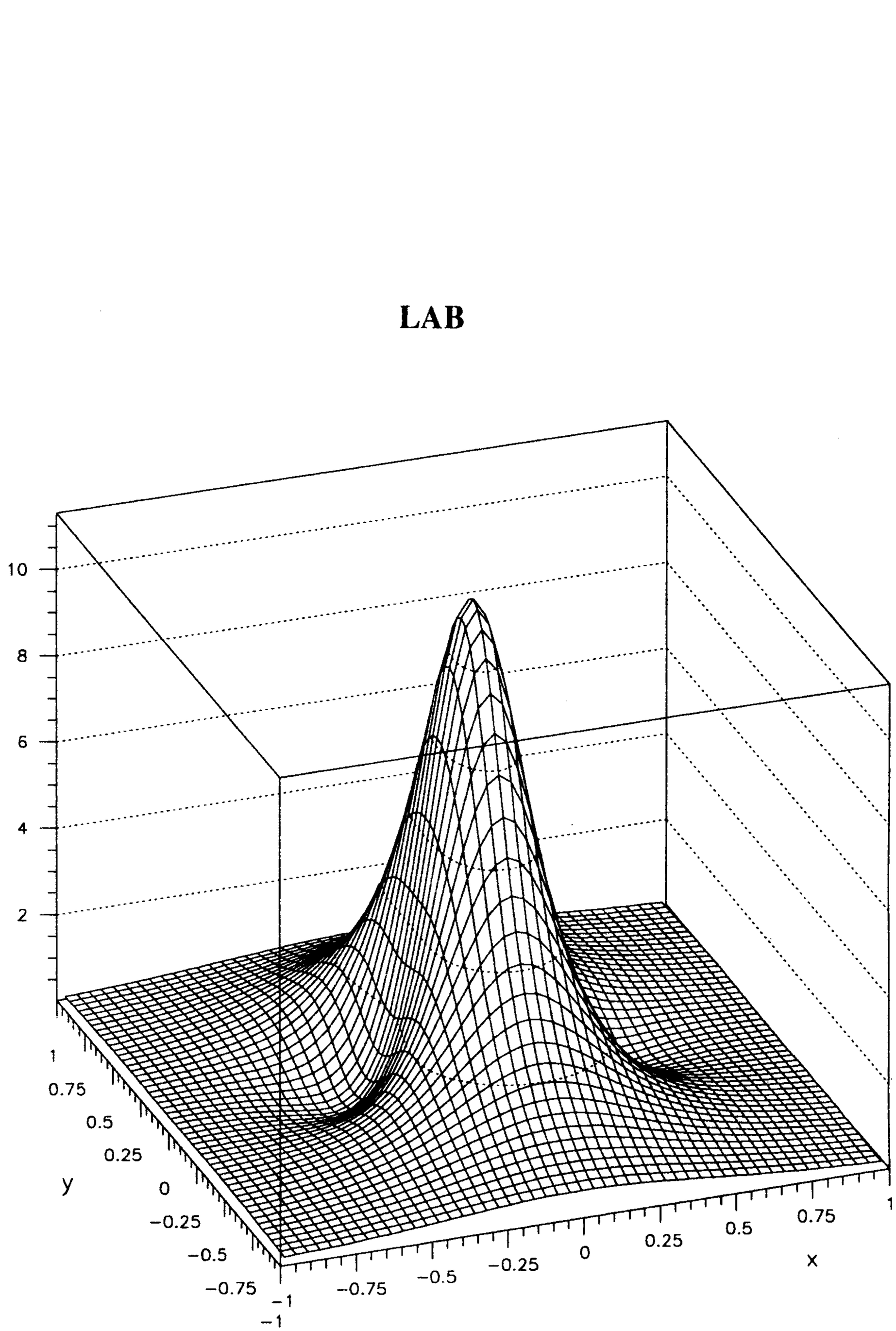

Figure 9: Klein-Nishina differential cross-section $d^2\sigma/dxdy$, in units of r_0^2, in a plane transverse to the photon momentum in the **LAB**-system. The polarization vectors of the incoming particles are $[\vec{s}^{(i)} = (0,0,1)]$ and $[\vec{\zeta} = 0]$, respectively. The unit circle in the (x,y) plane correspond to a cone of half-aperture $2/\gamma$.

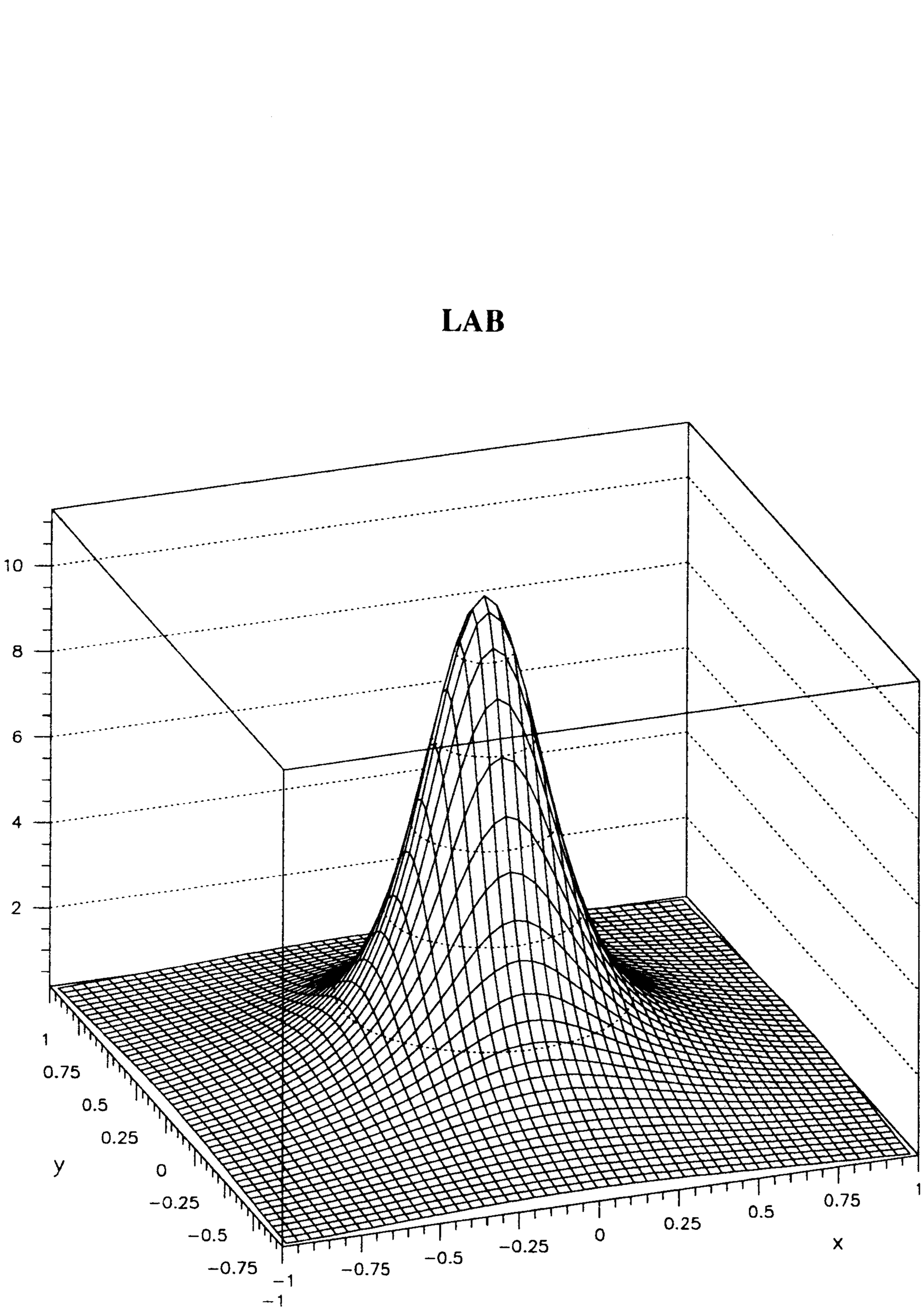

Figure 10: The same of fig.(9) for circularly polarized incoming photon $[\vec{s}^{(i)} = (0, 1, 0)]$.

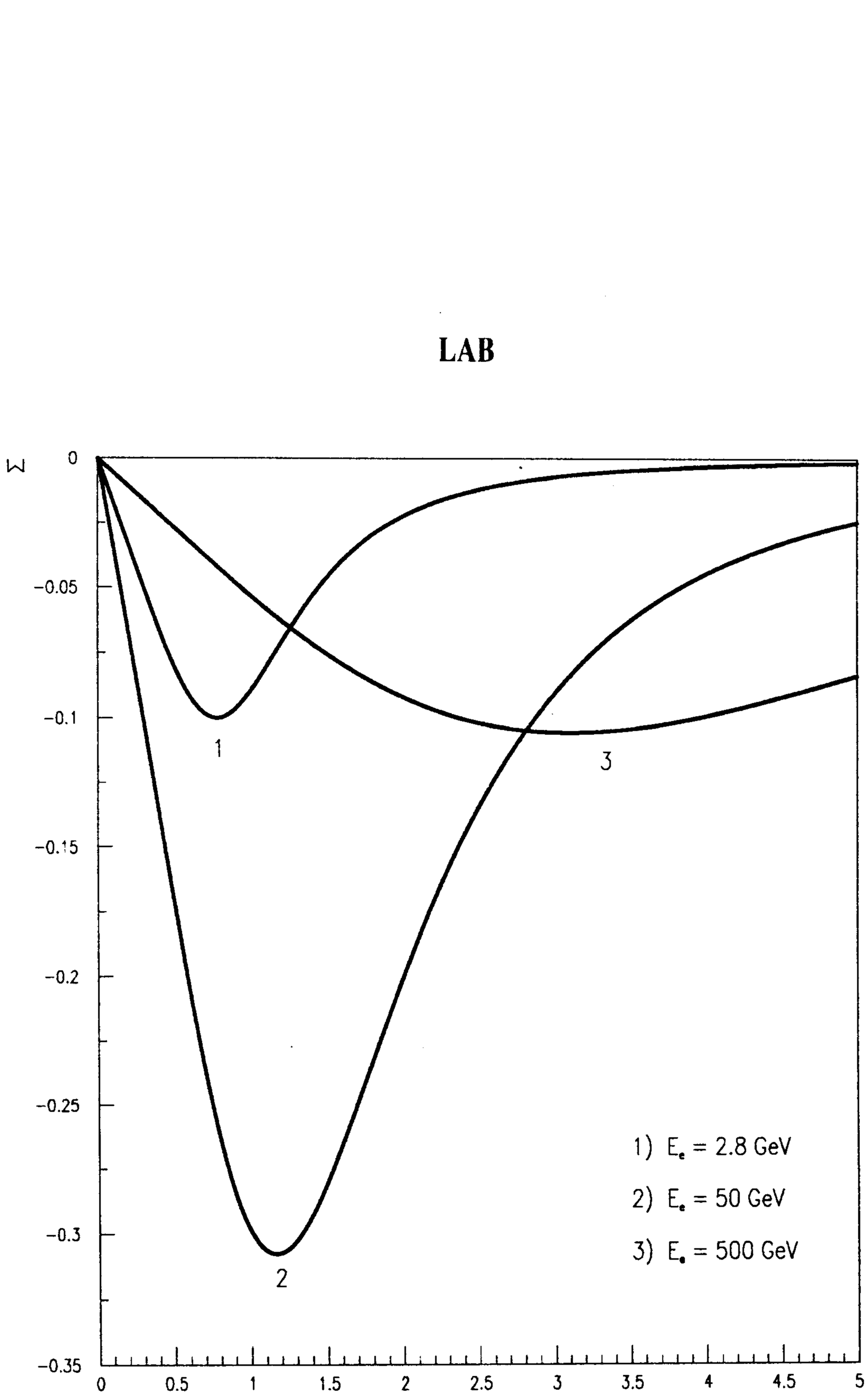

Figure 11: The asymmetry of fig.(5) as seen in the **LAB**-system. $\Delta\theta$ is the angle of the scattered photon with respect to the backward direction in units of $1/\gamma$.

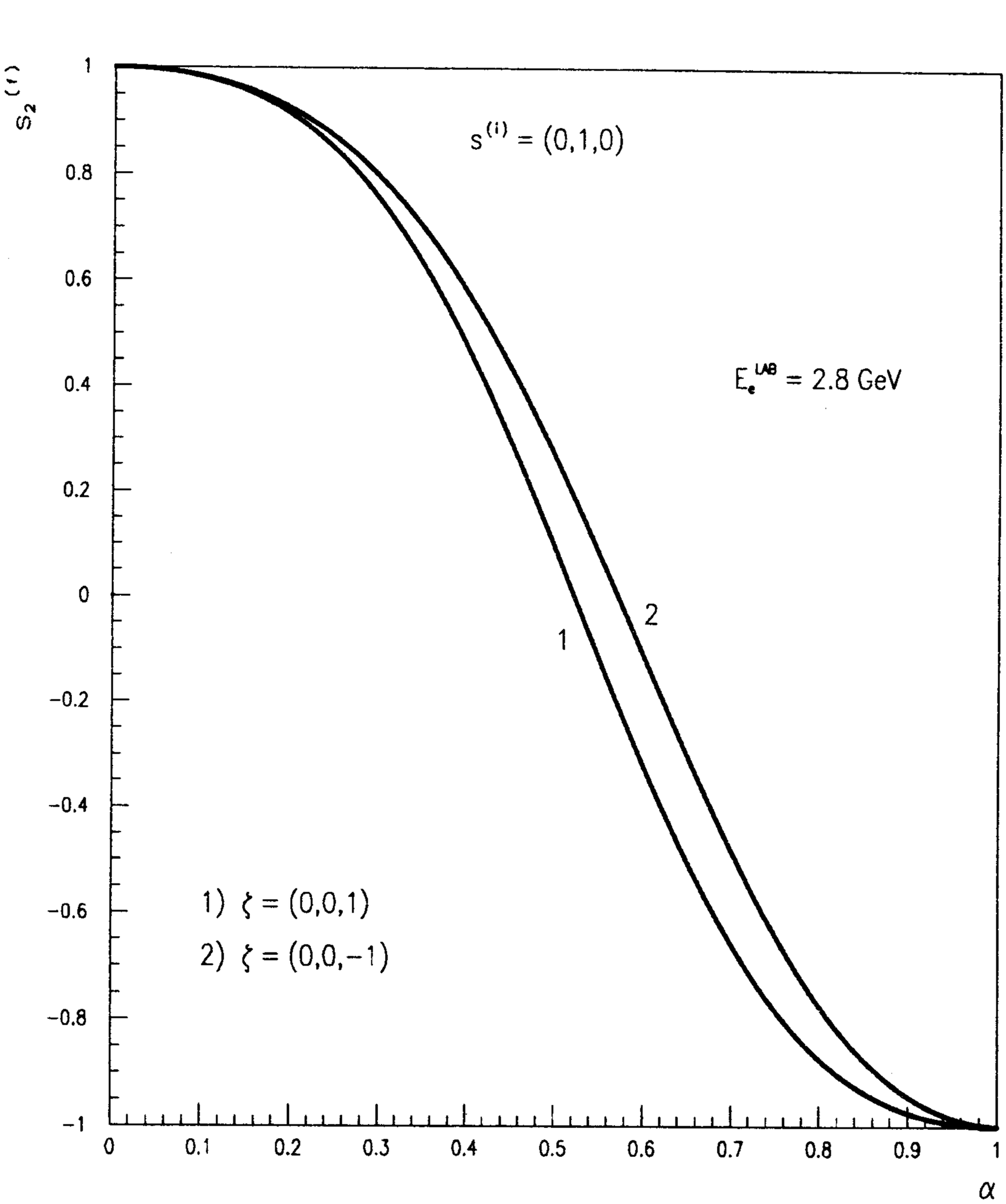

Figure 12: The same of fig.(7a) in the **LAB**-system.

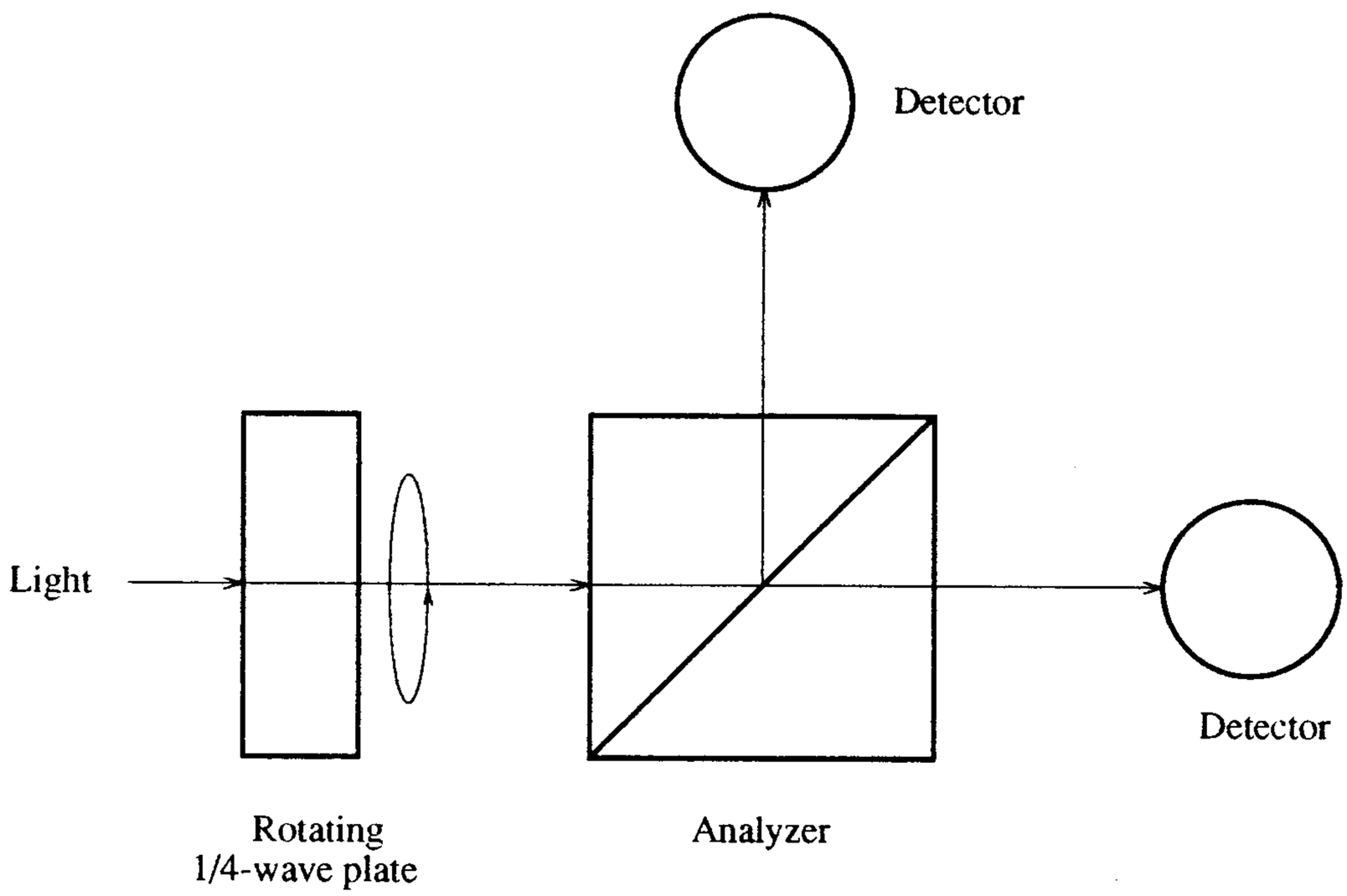

Figure 13: Experimental set-up for the polarization measurement.

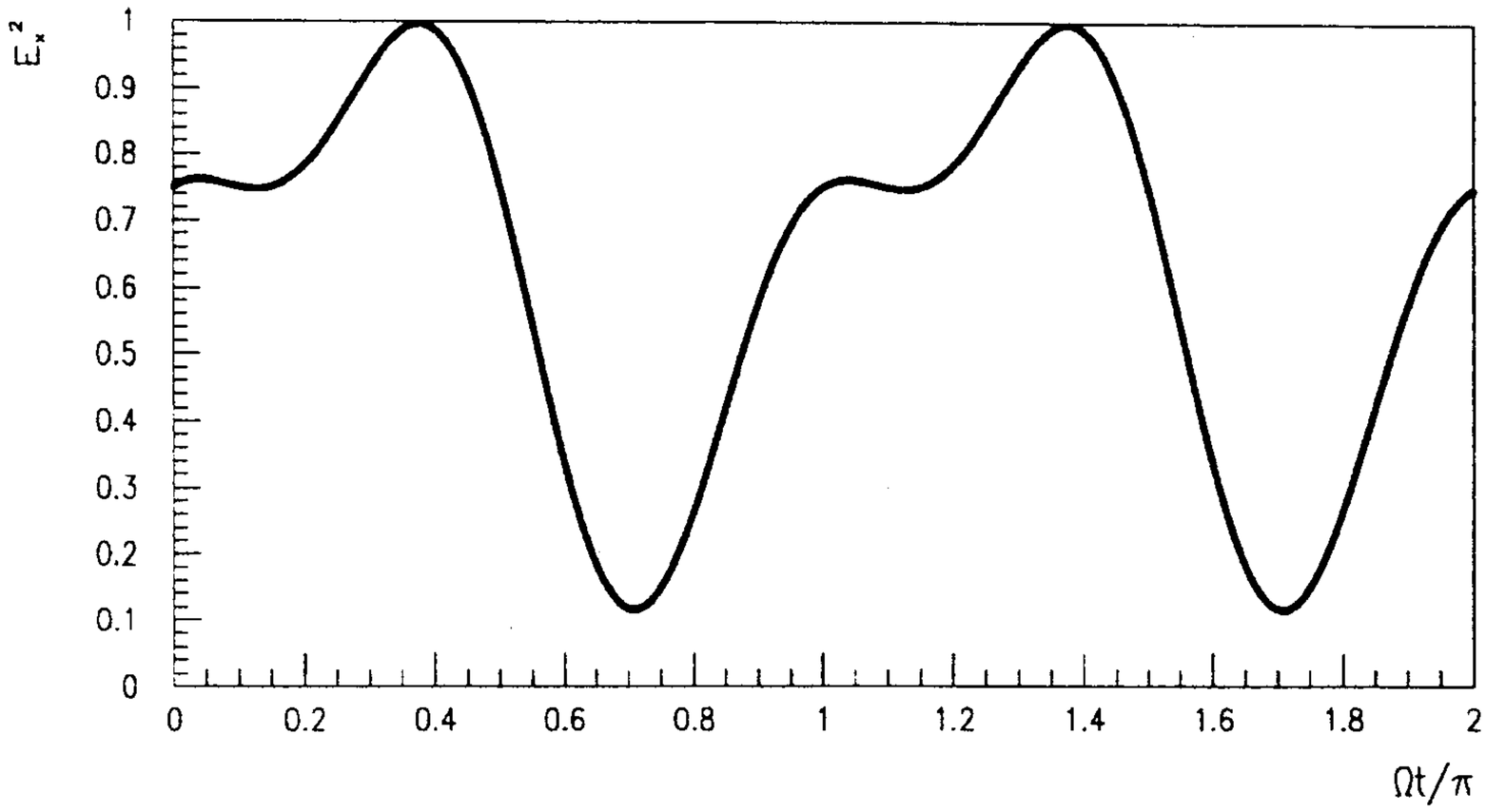

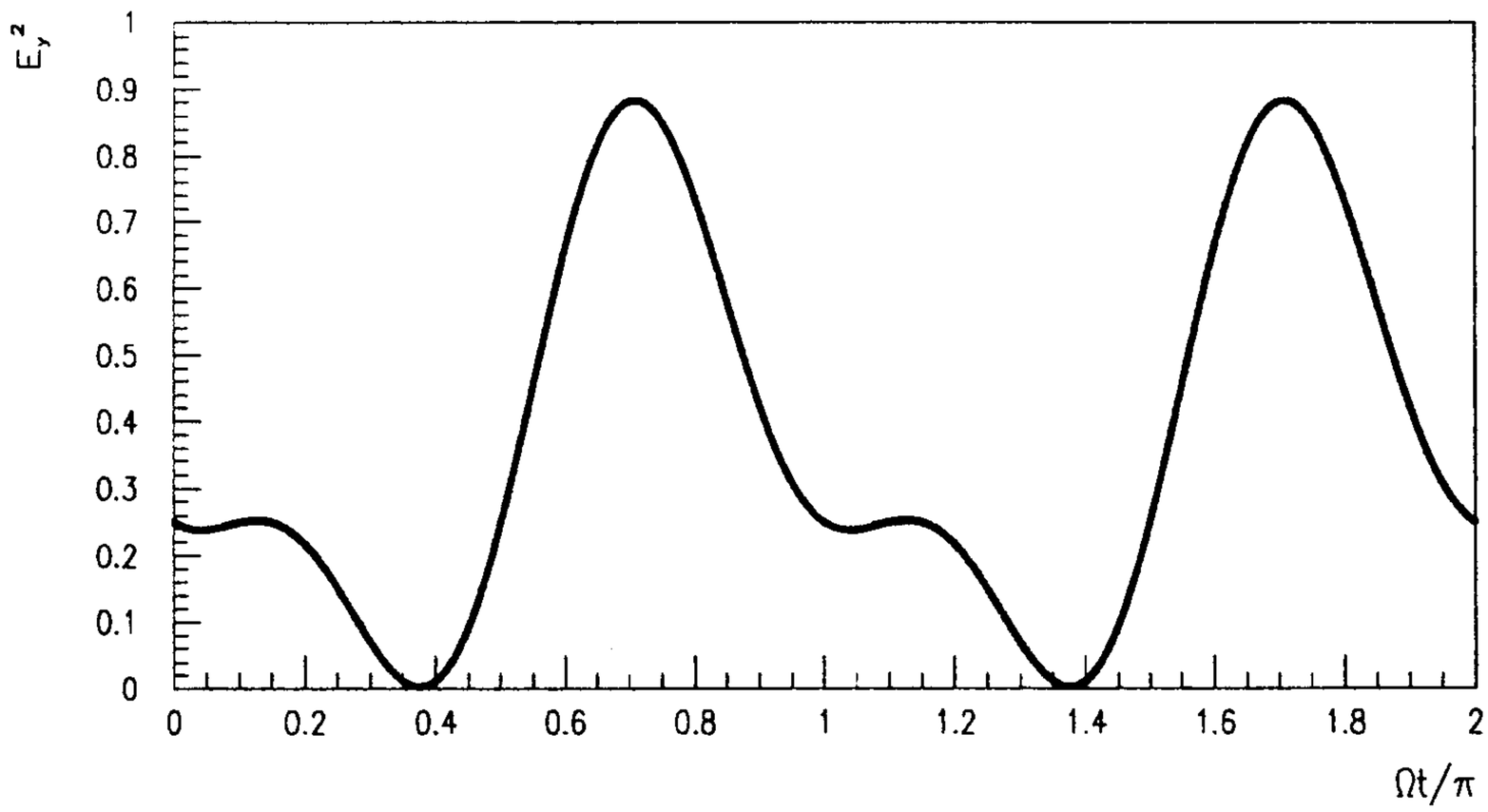

Figure 14: The intensities of eq.(4.4) as a function of the rotation angle of the plate in the case $\vec{\xi} = (0.5, 0.7, 0.5)$ $[P^2 = 0.99]$.